Science of the Total Environment 421–422 (2012) 253–259

Contents lists available at SciVerse ScienceDirect

Science of the Total Environment

journal homepage: www.elsevier.com/locate/scitotenv

# Contaminant mobility and carbon sequestration downstream of the Ajka (Hungary) red mud spill: The effects of gypsum dosing

P. Renforth [a,*], W.M. Mayes [b], A.P. Jarvis [c], I.T. Burke [d], D.A.C. Manning [c], K. Gruiz [e]

[a] Department of Earth Sciences, University of Oxford, South Parks Road, Oxford, OX3 0DP, UK
[b] Centre for Environmental and Marine Sciences, University of Hull, Scarborough, YO11 3AZ, UK
[c] School of Civil Engineering and Geosciences, Newcastle University, Newcastle upon Tyne, NE1 7RU, UK
[d] School of Earth and Environment, University of Leeds, Leeds, LS2 9JT, UK
[e] Department of Applied Biotechnology and Food Science, Budapest University of Technology and Economics, 1111 Budapest, St. Gellért sq. 4, Hungary

ARTICLE INFO

*Article history:*
Received 3 October 2011
Received in revised form 13 December 2011
Accepted 20 January 2012
Available online 19 February 2012

*Keywords:*
Bauxite processing residue
Red mud
Carbon dioxide removal
Stable isotope
Hyperalkaline wastes
Carbonate precipitation

ABSTRACT

A number of emergency pollution management measures were enacted after the accidental release of caustic bauxite processing residue that occurred in Ajka, western Hungary in October, 2010. These centred on acid and gypsum dosing to reduce pH and minimise mobility of oxyanion contaminants mobile at high pH. This study assessed the effectiveness of gypsum dosing on contaminant mobility and carbon sequestration through assessment of red mud and gypsum-affected fluvial sediments via elemental analysis and stable isotope analysis. There was a modest uptake of contaminants (notably As, Cr, and Mn) on secondary carbonate-dominated deposits in reaches subjected to gypsum dosing. C and O stable isotope ratios of carbonate precipitates formed as a result of gypsum dosing were used to quantify the importance of the neutralisation process in sequestering atmospheric carbon dioxide. This process was particularly pronounced at sites most affected by gypsum addition, where up to 36% of carbonate-C appears to be derived from atmospheric in-gassing of $CO_2$. The site is discussed as a large scale analogue for potential remedial approaches and carbon sequestration technologies that could be applied to red mud slurries and other hyperalkaline wastes. The results of this work have substantial implications for the aluminium production industry in which 3–4% of the direct $CO_2$ emissions may be offset by carbonate precipitation. Furthermore, carbonation by gypsum addition may be important for contaminant remediation, also providing a physical stabilisation strategy for the numerous historic stockpiles of red mud.



## 1. Introduction

The failure of the north-western corner of Cell X of the Ajkai Timfoldgyar Zrt alumina plant's bauxite processing residue (red mud) depository on the 4th October 2010 led to a sudden release of 600,000–700,000 $m^3$ of a highly caustic (pH 13) red mud suspension, which engulfed the downstream villages of Kolontár, Devecser and *Somlóvásàrhely* in western Hungary (Gruiz, 2010; Mayes et al., 2011). The disaster prompted the activation of the EU Civil Protection Mechanism to combat the effects of the pollutant release (European Commission Monitoring and Information Centre for Civil Protection, 2010). Immediate emergency management focussed on the removal of red mud from residential areas and in some cases the ploughing of thin surface deposits into underlying soils to minimise dust-blown hazards (Gruiz, 2010; Gelencsér et al., 2011). Water management initially focussed on neutralising pH through dosing with acid (acetic, hydrochloric, nitric) and gypsum throughout the Torna Creek and the Marcal and Rába rivers, prior to the outlet of the Rába system to the Danube. Water jets were used to aid gypsum mixing with high pH waters and were effective in limiting pH to levels below 10.5 in lower reaches of the Marcal River soon after the spill (Hungarian Ministry of Foreign Affairs, 2010). Residual releases of red mud suspension from the breached cell were also a remedial priority, through the construction of a Permeable Reactive Barrier (PRB) from the fly ash that previously comprised the wall, and of a series of settlement lagoons to minimise solids transport downstream from source zones (Gruiz, 2010; Mayes et al., 2011). Longer term efforts have seen a semi-permanent, automated, acid dosing station built near the original depository. Red mud deposited on the flood plain of the Torna Creek has been successfully recovered and stored in a newly constructed impoundment with improved structural integrity (Reeves et al., 2011).

Initial studies on the environmental effects of the spill have found that on floodplain soils inundated with red mud, salinity and high alkalinity rather than contaminant element enrichment is the key constraint to plant growth (Ruyters et al., 2011), a finding consistent with the broad body of restoration ecology literature on the rehabilitation of red mud disposal sites (e.g. Gräfe and Klauber, 2011). Preliminary studies on the fluvial sediment contamination have highlighted the abundance of vanadium, chromium, nickel and

* Corresponding author.
*E-mail address:* Phil.Renforth@earth.ox.ac.uk (P. Renforth).

0048-9697/$ – see front matter © 2012 Elsevier B.V. All rights reserved.
doi:10.1016/j.scitotenv.2012.01.046

arsenic downstream of the spill, although the bulk of these potential contaminants (with the exception of V) appear to be associated principally with hard-to-leach residual phases that are unlikely to be mobile in the environment (Mayes et al., 2011). The fine grain size of the released material also lends itself to transport downstream and rapid dispersion (Mayes et al., 2011). Speciation studies have reinforced these patterns (Burke et al., 2011), but also highlighted the prevalence of vanadium in mobile pentavalent species (the most toxic form of V), which may be leached from red mud after deposition on floodplain areas.

Gypsum has been widely used as an ameliorant or soil amendment at bauxite processing residue (the fine fraction of which is referred to as red mud) disposal sites (e.g. Courtney and Timpson, 2005; Wehr et al., 2006; Gräfe and Klauber, 2011). The addition of gypsum provides $Ca^{2+}$ which displaces $Na^{+}$ from exchange complexes and reduces salt stress to vegetation (Gräfe and Klauber, 2011). The $Ca^{2+}$ addition also serves to regulate pH and helps buffer the highly caustic (alkalinity >20,000 mg/L as equivalent $CaCO_3$: Johnston et al., 2010) red mud substrate to within the range tolerable by plants (Gräfe and Klauber, 2011). In hyperalkaline conditions, atmospheric $CO_2$ readily in-gasses into waters (Roadcap et al., 2005) and reacts with the hydroxyl ion (abundant in the Bayer liquor from use of NaOH ore digestant) to form bicarbonate (Eq. 1a). The addition of gypsum to red mud leachate provides free $Ca^{2+}$, prompting precipitation of calcium carbonate (Eq. 1b) which consumes alkalinity and lowers pH (thermodynamic data from Robie and Hemingway, 1995). Other precipitation products formed through gypsum addition to red mud slurries include tricalcium aluminate ($Ca_3Al_2O_6$), Portlandite ($Ca(OH)_2$) and hydrocalumite ($Ca_2Al(OH)_7.2H_2O$; Gräfe et al., 2011). This buffering process, ubiquitous in hyperalkaline waters containing the weathering products of portlandite (e.g. steel slag and some fly ash leachates: Mayes et al., 2009), is otherwise limited in red mud leachates by the lack of dissolved $Ca^{2+}$ and $Mg^{2+}$ prior to gypsum addition.

$$OH^-_{(aq)} + CO_{2(aq)} \rightarrow HCO_3^-{}_{(aq)} \quad (1a)$$

$$2OH^-_{(aq)} + CaSO_4.2H_2O_{(s)} + 2CO_2 \leftrightarrow CaCO_{3(s)} + SO_4^{2-}{}_{(aq)} + 2H_2O_{(l)} + H_2CO_{3(aq)} \quad \Delta Gr = -692.5 kJ/mol \quad (1b)$$

Silicate-bearing waste materials may be able to sequester atmospheric $CO_2$ on human relevant time scales at globally significant quantities (Renforth et al., 2011), and red mud has been suggested to be suitable in this context (Yadav et al., 2010). Existing investigations of mineral carbonation have shown that the carbon capture potential of a material is dependent on the quantity of non-carbonated divalent cations (predominantly Ca and Mg) and the reactivity of the phase in which they are situated. For instance, iron and steel slags have a typical MgO + CaO content >50%, primarily as amorphous glasses, and have been shown to sequester atmospheric carbon dioxide under ambient temperatures and $pCO_2$ (Renforth et al., 2009).

Through employing isotopic analyses alongside a range of geochemical investigations, this paper assesses the efficacy of gypsum dosing as part of emergency management with regard to the mobility of contaminants downstream of the Ajka red mud spill. The processes taking place also provide a useful, large-scale analogue to potential remedial interventions and carbon capture mechanisms at sites managing hyperalkaline slurries produced in the Bayer Process.

## 2. Methods

Sediment samples were collected from a series of stations across the 3072 $km^2$ Marcal river system on the 30th November and 1st December 2010 (see Mayes et al., 2011 for detail). At each station triplicate bulk (~500 g) sediment samples were collected by aggregating three randomly collected sub-samples from a 12 $m^2$ area of stream bed (9 separate locations sampled at each reach to give three replicates). Additional spot samples from stock-piled gypsum deposits (at location M4: Fig. 1), gypsum-affected fluvial sediments (M4), and floodplain deposits of transported red mud at *Somlóvásàrhely (S1)*.

Sediments were homogenised, air-dried, disaggregated gently and sieved (2 mm aperture) prior to microwave-assisted total digestion (aqua regia and HF) following the method of USEPA (1996). Major and minor element concentrations in digests and extracts were determined using a Perkin Elmer Elan DRCII inductively Coupled Plasma-Mass Spectrometer (ICP-MS; for As, Cr and Mo) and an Optima 5300 DV ICP-OES for all other elements.

Calcium carbonate content was determined using an Eijkelkamp calcimeter (BS 7755-3.10:1995). C and O stable isotope ratios were determined on selected samples by Iso-Analytical Ltd, Crewe, UK (http://www.iso-analytical.co.uk/). Carbonate samples were digested in pure phosphoric acid and isotope ratios were measured on the evolved $CO_2$ using a Europa Scientific 20–20 isotope ratio mass spectrometer calibrated against standards NBS-19, IA-R022 and NBS-18. The mean of the standards was consistently within one standard deviation of the accepted value and analytical precision was ±0.05‰ for $\delta^{13}C$ and ±0.07‰ $\delta^{18}O$, referred to Vienna-Pee Dee Belemnite (VPDB).

Samples of the stockpiled material were analysed using a Netzsch STA449C TG-DSC (thermogravimetry-differential scanning calorimetry, or TG-DSC) system with an atmosphere of flowing (30 ml/min)

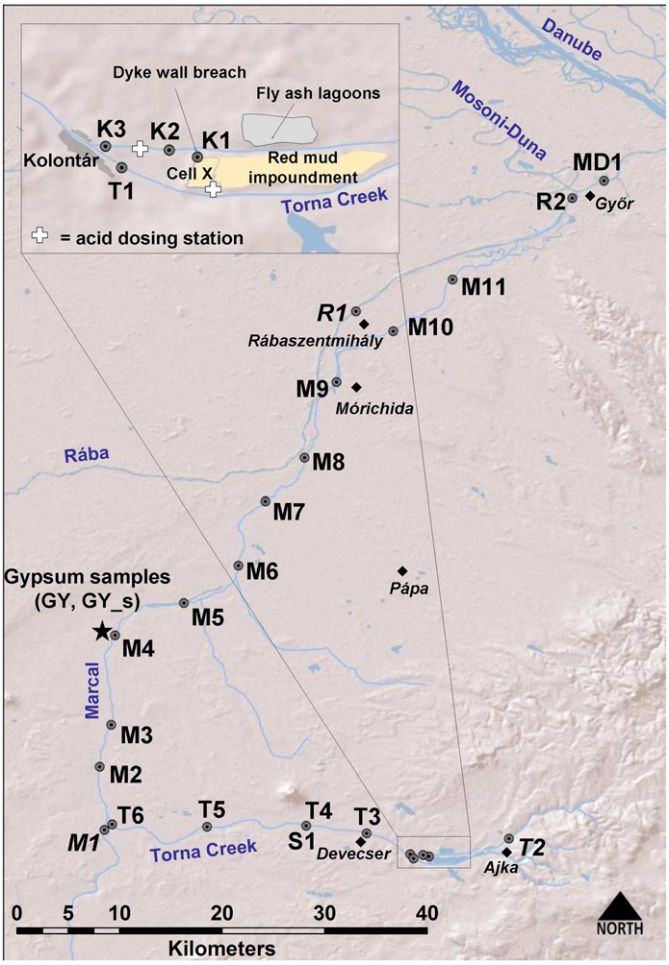


**Fig. 1.** Location map of sample stations (circles) across the Marcal and Rába catchments. Population centres shown with a diamond. Reference site labels in italics.

80% He, 20% $O_2$, in, connected to a Netzsch Aeolos 403 C quadrupole mass spectrometer (QMS; m/z range 10–300). Samples were loaded into alumina crucibles (approximately 30–40 mg sample mass). A heating rate of 10 °C min-1 was used from 0 to 1000 °C.

Principal Component Analysis and all other statistical analyses were undertaken in Minitab v15. PCA was undertaken on standardised total extraction data to examine the evolution of bulk geochemistry with distance from the site and the relative mixing of red mud with fluvial sediments. Data were not normally distributed even after log-transformation (Kolmogorov–Smirnov $p > 0.05$) so non-parametric methods were used. Hydrochemical data from Mayes et al. (2011) and CSIRO (2009) were analysed using the geochemical code PHREEQC v.1.5.10 (Parkhurst and Appelo, 1999) with the WATEQ4F database (Ball and Nordstrom, 1991).

## 3. Results and discussion

### 3.1. Trace element attenuation

Bulk elemental analysis of the sediments collected highlights a dilution gradient of red mud downstream from source areas (rich in Al, Na, As, Cr, Ni, V and rare earth elements: REE; Table 1) which provide an end-member of the most affected area adjacent to the cell (K1), to unaffected sites which are relatively enriched in elements indicative of lithogeneous sources (e.g. Ba, Mg, K: Mayes et al., 2011). Although hotspots of red mud enrichment are apparent up to around 60–70 km downstream of Ajka (e.g. M2, M4) the signal of red mud deposition is difficult to distinguish from reference sites at sample stations in lower Marcal (e.g. M7) and those in the Raba (R2) and Mosoni Duna, towards the confluence with the Danube. The signal of gypsum addition on fluvial sediments is also stark (Fig. 2), with elevated Ca and S relative to source red mud samples and unaffected sites (Table 1). Total sulphur is a particularly good indicator of gypsum amendment in the system given theoretical concentrations in gypsum exceeds 186 g/kg while reference sites have total sulphur content between 182 and 552 mg/kg, and source material (K1) ranges between 2750 and 2894 mg/kg. A gradient of mixing from theoretical gypsum to gypsum-affected stream sediments (e.g. M7, M9-11) is apparent in the upper left of Fig. 2. The addition of gypsum was evident at numerous sample stations where the streambed was blanketed in gypsum-rich sludges and secondary carbonate precipitates, or where high stage marks on downstream bridge piers suggested recent carbonate precipitation. These were predominantly on the Marcal river, but stations at K3, T3 and T6 on the Torna Creek also exhibit elevated S concentrations elevated above impoundment samples and reference samples suggesting significant localised gypsum addition (Table 1; Fig. 2).

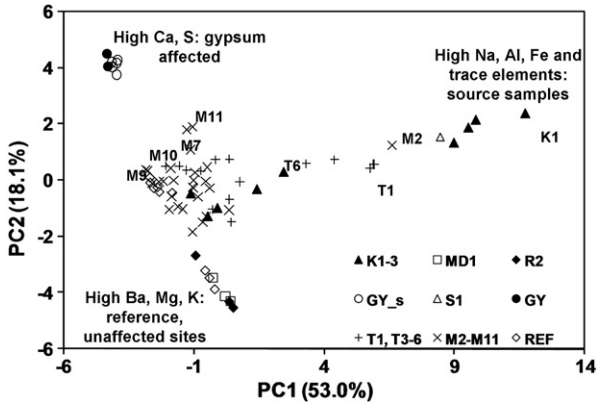


**Fig. 2.** Principal Component Analysis of sediment total elemental composition data by site (after Mayes et al., 2011). Ordination of sample sites by the first two principal components is displayed. GY: stockpiled gypsum; GY_s: instream gypsum deposits; S1: floodplain sample adjacent to T4.

Analysis of the gypsum-amended instream sediments suggests some modest trace element uptake relative to adjacent stockpiled samples (Table 2). For some of the more mobile elements downstream of the impoundment (As, Cr, V: see Mayes et al., 2011) this difference is statistically significant, albeit obtained from a small sample size. Whether this reflects uptake of such elements within secondary deposits and gypsum, or capture of colloidal red mud

**Table 1**
Mean composition of digested (aqua regia/HF) fluvial sediments ($n = 3$) at selected sample stations on the Torna Creek and Marcal River (after Mayes et al., 2011). All values in mg/kg. Reference samples M1, R1 and T2 shown on right hand side (italics). S1: floodplain deposit from Somlóvásàrhely; G: stoichiometric concentrations of Ca and S in pure gypsum.

| Element | K1 | K3 | T1 | S1 | M4 | M7 | M10 | *M1* | *R1* | *T2* | *G* |
|---|---|---|---|---|---|---|---|---|---|---|---|
| Distance from spill (km) | 0 | 1.5 | 1.6 | 9.4 | 44.7 | 64.2 | 85.9 | 25.8 | 100.0 | −6.3 | 44.7 |
| Ca | 53500 | 79100 | 79900 | 47900 | 73000 | 135000 | 81300 | 17000 | 10400 | 40400 | 232600 |
| Mg | 2982 | 7111 | 8733 | 3674 | 7718 | 19100 | 7370 | 3859 | 8351 | 10530 | – |
| K | 737 | 5543 | 5476 | 2637 | 5239 | 5758 | 9119 | 8166 | 18662 | 9235 | – |
| Na | 39920 | 19390 | 21980 | 43220 | 26120 | 2969 | 4401 | 5350 | 9760 | 9522 | – |
| Fe | 210300 | 113500 | 141600 | 174400 | 29300 | 11100 | 16400 | 11100 | 34800 | 13100 | – |
| Al | 75200 | 56300 | 59600 | 65300 | 59000 | 54900 | 37300 | 22800 | 66500 | 27300 | – |
| Si | 27900 | 75900 | 65000 | 47700 | 66000 | 113000 | 184700 | 339300 | 165200 | 54700 | – |
| S | 2692 | 3050 | 2262 | 2545 | 861 | 3887 | 4965 | 155 | 458 | 139 | 186000 |
| As | 78.5 | 51.9 | 54.3 | 61.3 | 52.8 | 45.4 | 14.9 | 5.8 | 3.1 | 1.7 | – |
| Ba | 59.8 | 168.4 | 134.3 | 52.0 | 121.7 | 189.2 | 203.4 | 183.7 | 448.3 | 163.9 | – |
| Cd | 4.0 | 1.7 | 2.1 | 2.7 | 2.0 | 1.6 | <1 | <1 | <1 | <1 | – |
| Ce | 473.2 | 254.8 | 264.8 | 422.5 | 285.4 | 7.3 | 17.8 | 25.5 | 54.2 | 27.5 | – |
| Co | 97.1 | 52.4 | 54.1 | 85.3 | 58.0 | 6.1 | 9.1 | 6.0 | 10.2 | 8.5 | – |
| Cr | 810.7 | 372.6 | 422.6 | 592.8 | 416.3 | 27.7 | 37.3 | 30.3 | 49.2 | 29.2 | – |
| Cu | 60.3 | 42.6 | 40.5 | 47.6 | 40.1 | 21.2 | 21.9 | 9.3 | 25.4 | 15.1 | – |
| Ga | 79.3 | 52.9 | 53.4 | 69.0 | 54.7 | 39.6 | 33.7 | 8.9 | 27.3 | 13.0 | – |
| Li | 57.5 | 60.5 | 54.9 | 65.3 | 58.6 | 20.9 | 23.0 | 12.7 | 40.9 | 13.6 | – |
| Mn | 2565.8 | 1606.8 | 1538.7 | 2462.3 | 1702.0 | 1855.3 | 1327.0 | 292.8 | 976.5 | 420.8 | – |
| Mo | 14.4 | 7.3 | 10.1 | 11.2 | 9.5 | 10.6 | 10.3 | 7.7 | 5.0 | 5.4 | – |
| Ni | 291.7 | 140.7 | 153.5 | 246.0 | 162.5 | 12.3 | 19.2 | 12.5 | 33.5 | 7.6 | – |
| Pb | 79.8 | 39.6 | 41.0 | 68.1 | 44.1 | 2.8 | 4.9 | 1.3 | <1 | 2.6 | – |
| Sr | 290.2 | 235.0 | 246.7 | 299.1 | 256.4 | 335.9 | 204.1 | 91.5 | 100.6 | 124.3 | – |
| Ti | 24800 | 12400 | 15000 | 21500 | 3721 | 1009 | 1557 | 1692 | 4718 | 3665 | – |
| V | 891.2 | 458.9 | 488.3 | 743.2 | 510.3 | 133.7 | 86.1 | 28.9 | 65.9 | 34.4 | – |
| Zn | 173.2 | 104.3 | 112.0 | 132.0 | 108.8 | 50.7 | 77.4 | 26.3 | 93.8 | 26.6 | – |
| Zr | 628.9 | 323.1 | 341.4 | 531.8 | 360.2 | 13.8 | 22.3 | 18.4 | 37.0 | 35.1 | – |

**Table 2**
Median and range (in parenthesis) in selected major and minor element concentrations (mg/kg) in stockpiled gypsum and gypsum-amended fluvial sediments taken from sample location M4 (n = 6 for stockpiled gypsum, n = 7 for secondary deposits.

| Site | As | Cr | Cu | Mn | Ni | S | V | Zn |
|---|---|---|---|---|---|---|---|---|
| Stockpiled gypsum | 13.3 (10.0–28.5) | 3.7 (2.8–5.2) | 3.0 (1.7–4.1) | 16.0 (6.0–27.4) | 1.9 (1.0–5.5) | 235300* (152300–248100) | 2.3 (1.1–3.5) | 7.5 (4.4–9.2) |
| Secondary instream calcareous deposits | 31.5* (12.5–45.0) | 6.4* (4.1–14.4) | 2.4 (1.7–5.22) | 54.3* (18.6–106.4) | 2.9 (1–7.8) | 151800 (123100–223800) | 4.9* (3.2–19.6) | 9.7 (3.1–18.5) |

* Median is significantly higher at $p<0.05$ using Mann Whitney U test).

fines transported downstream of the site is uncertain sequential extraction of affected fluvial sediments at the site suggested a greater relative importance of NaOAc / HOAc and NH2OH.HCl extractable phases (in the operationally defined Tessier et al. (1979) scheme) of As, Ni and V at sites subject to gypsum dosing than source sediments (Mayes et al., 2011). This could support the notion of scavenging by gypsum and neo-formed carbonate deposits but further analysis would be required to elucidate specific modes of attenuation. It should be noted that due to the potential precipitation of $CaF_2$ during aqua regia-HF acid digestion, the accuracy of the values reported for Ca in Table 1 is limited. For this reason, total S concentration has been used to understand gypsum addition in the catchment.

### 3.2. Stockpiled gypsum analysis

The purity of the stockpiled gypsum was confirmed using thermogravimetric analysis in which a 15–18% mass loss was recorded at 150 °C which is indicative of gypsum dehydration. Varying weight loss (3–7%) was recorded at 700 °C, indicative of calcium carbonate decarbonation. This suggests that the sample is approximately 71–86% gypsum and 7–16% calcium carbonate. X-ray diffraction analysis (XRD) confirmed that gypsum and calcite are the predominant phases in the sample.

### 3.3. Stable isotope data

C and O stable isotope ratios in carbonates have been used to investigate the provenance of the elemental components and the condition of the environment from which they form (e.g. Hudson, 1977). There is a distinctive isotopic composition in carbonates formed from high pH solutions associated with waste silicate materials such as cement (Dietzel et al., 1992; Krishnamurthy et al., 2003; Macleod et al., 1991), lime waste (Andrews et al., 1997), iron and steel slag (Renforth et al., 2009) and ashes (Fléhoc et al., 2006; see Fig. 3). The light $\delta^{13}C$ isotopic signatures are explained using the interpretation proposed by Usdowski and Hoefs (1986), who suggest an isotopic enrichment factor of $\delta^{13}C$ (Eq. 2) in carbonate and dissolved $CO_2$ during the reaction shown in Eq. 1a.

$$\varepsilon_{CaCO3-CO2} = -18.8‰ \quad (2)$$

The carbonate mineral $\delta^{18}O$ in high pH solutions is a mixture of $\delta^{18}O$ produced from the fractionation between hydroxide and meteoric water, and atmospheric $CO_2$ according to Eqs. 3 and 4 (Dietzel et al., 1992; Usdowski and Hoefs, 1986; Létolle et al., 1990):

$$\delta^{18}O_{CaCO_3} = \frac{1}{3}\delta^{18}O_{OH^-} + \frac{2}{3}\delta^{18}O_{CO_2} \quad (3)$$

$$\varepsilon_{OH^- - H_2O = -42‰} \quad (4)$$

This is generally consistent with the low O isotope ratios reported in the literature (Andrews et al., 1997; Clark et al., 1992; Fléhoc et al., 2006; Kosednar-Legenstein et al., 2008; Krishnamurthy et al., 2003; Macleod et al., 1991; O'Neil and Barnes, 1971; Renforth et al., 2009; van Strydonck et al., 1989). The influence of atmospheric carbon and $\varepsilon_{OH-H2O}$ in Eqs. 3 and 4 reduces the effect of $\delta^{18}O$ meteoric water variation between −50 and −35‰ to precipitate carbonates in high pH solutions with $\delta^{18}O$ between a smaller range of −24 and −19‰. This approach provides a useful tool in highlighting the importance of secondary carbonates as a carbon sink.

Carbonate stable isotope ratios were $-12.80‰ \leq \delta^{13}C \leq -3.54‰$, and $-12.37‰ \leq \delta^{18}O \leq -8.03‰$. Isotope ratios were more negative adjacent to the storage facility (points K3, S1 and T1 had $\delta^{13}C$ between −10.90‰ and −12.40‰, and $\delta^{18}O$ between −10.38‰ and −12.37‰). In contrast, carbonate isotope ratios adjacent to the confluence between the Mosoni-Duna and the Danube (MD1 and R2) are more consistent with those in the Triassic limestone bedrock ($\delta^{13}C = -3.5‰$, $\delta^{18}O = -1.7‰$; Pálfy et al., 2001)

Assuming that atmospheric $CO_2$ is the only source of carbon in hydroxylation isotopic fractionation, the proximity of the isotope values in the samples to end members can be used to determine the quantity of sequestered atmospheric $CO_2$. Hydroxylation will produce an end

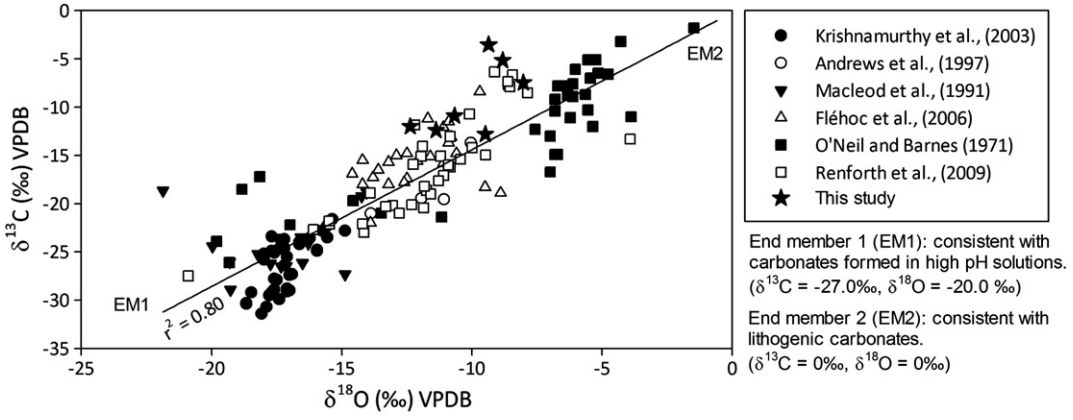


**Fig. 3.** Isotopic ratios of carbonates formed in high pH environments. The line denotes linear mixing of carbonates between hydroxylation and lithogenic carbonate end members. Analytical error is within the size of the data points.

member with an isotopic ratio of −27.0‰ for $\delta^{13}C$, and −20.0‰ for $\delta^{18}O$ (assuming meteoric water $-37.5‰ \leq \delta^{18}O \leq -35.2‰$; Bajnóczi and Kovács-Kis, 2006). Therefore, it is estimated that between 10.5 and 38.1 ± 0.6% of the carbon in the carbonate is derived from the atmosphere and the remaining carbonate is derived from lithogenic sources (Table 3).

There is a strong, significant positive correlation ($r_s = 0.94$; $p = 0.005$) between total S content of the sample and the proportion of carbon derived through hydroxylation of atmospheric $CO_2$ (Fig. 4). This suggests the greater influence of secondary carbonate deposits at the heavily gypsum-dosed sites, as would be anticipated given the addition of non-carbonated divalent cations (notably $Ca^{2+}$, $Mg^{2+}$ and $Sr^{2+}$: Table 1). The relationship does not reflect the downstream gradient in pH that was apparent shortly after the spill (ECMICCP, 2010) or the sharper pH gradient from residual releases in the months after (Mayes et al., 2011). While there are samples with a high proportion of atmospheric carbon in the deposits in source areas (e.g. K3, T1), and the lowest proportion towards the largely unaffected sites at the catchment outlet (R2, MD1), there is a particular hotspot of gypsum enrichment (and enhanced carbonate crust formation indicative of atmospheric sources) at site M11. This site lies around 15 km downstream of a temporary gypsum storage depot which was a focus for coordinating dosing efforts in the spill aftermath at Mórichida (Hungarian Ministry of Foreign Affairs, 2010) and was particularly gypsum-rich. Sample S1 (transported red mud) has relatively elevated S, reflecting the influence of the source term (Table 1), while the relative elevation of the atmospherically-derived carbon at the transported red mud sample S1 may reflect the carbonation apparent in surface deposited red mud which gets at least partially neutralised over time (Gräfe et al., 2011).

### 3.4. PHREEQC modelling results

To understand the effect of gypsum addition on the saturation state of carbonate minerals in red mud leachate solutions, a model was constructed in PHREEQC using solution chemistry data from Mayes et al. (2011) for sample points K1, K2 and K3 and laboratory leaching results (CSIRO, 2009), which are indicative of solutions in contact with red mud. The results (Table 4) show that solutions in equilibrium with gypsum are more saturated with respect to calcite and aragonite. While solution pH is directly reduced by gypsum addition as seen in Table 4, carbonate precipitation (resulting in the dissolution of additional $CO_2$ and the deprotonation of $H_2CO_3$) is probably the key pH reduction mechanism in the environment which is not shown in static equilibrium models.

## 4. Conclusions and management implications

The acid neutralising capacity of red mud is approximately 10 mol/kg, equivalent to a reduction in $[H^+]$ or an increase in $[OH^-]$. Eq. 1a and 1b suggest that 1 mol of gypsum is required to neutralise 2 mol of $OH^-$ and form 1 mol of $CaCO_3$. Therefore, every tonne of red mud requires approximately 860 kg of gypsum, which would capture approximately 220 kg of $CO_2$. Between 60 and 120 Mt of red mud is produced annually (Ruyters et al., 2011; Yadav et al., 2010; Liu et al., 2007), which could be treated with 52–103 Mt of gypsum (33–69% of current global crude and synthetic gypsum production; USGS, 2010) and sequester 13–26 Mt of $CO_2$ (3–4% of $CO_2$ emissions from primary aluminium production; (Harnisch et al., 1998; USGS, 2011)). The global inventory of red mud may be approximately 2600 Mt (Power et al., 2011), which may have a carbon capture potential of 572 Mt $CO_2$. The large scale extraction, processing, and transport of gypsum is indicative of other carbon reduction geoengineering technologies (see The Royal Society, 2009) and may be coupled to the desulphurisation process on coal fired power stations as has been successfully deployed elsewhere (e.g. Yamada and Harato, 1982; Leoni and Penco, 2002). However, a comprehensive cost benefit analysis, which includes the reduced risk of contamination, is required to access the feasibility of treating red mud in this way. This gypsum dosing method may be suitable for other industries with NaOH bearing waste streams including 'black liquor' in paper manufacturing,

Gypsum has been widely applied in ameliorating the high alkalinity of bauxite residue slurries and solids (Courtney and Timpson, 2005; Gräfe et al., 2011). The emergency management in the aftermath of the Ajka spill represents the largest-scale field application of gypsum to red mud leachate-affected surface waters. The gypsum dosing was deemed effective in buffering the high pH waters after the initial release (Hungarian Ministry of Foreign Affairs, 2010) and secondary deposits have sequestered both trace contaminants and atmospheric carbon in demonstrable quantities. Gypsum is also currently being used in new waste stockpiling and stabilisation procedures at Ajka (Benedek, 2011). As such, gypsum addition may represent an avenue for future experimentation under controlled conditions to develop long-term buffering alternatives to direct acid

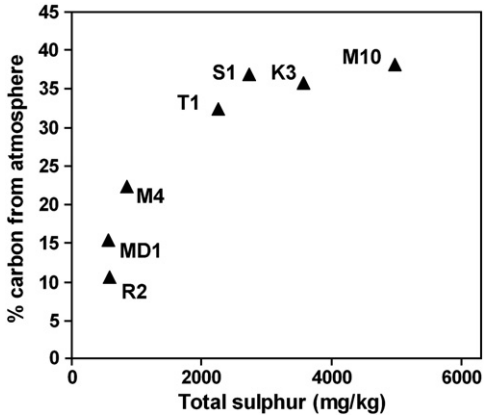


**Fig. 4.** Total sulphur content (mean of 3 samples) versus the proportion of carbon estimated to be derived from hydroxylation of atmospheric carbon.

**Table 3**
Isotopic ratios of samples and % of carbon derived from the atmosphere.

| Sample | Distance from source (km) | $\delta^{13}C_{V\text{-}PBD}$ (‰) | $\delta^{18}O_{V\text{-}PBD}$ (‰) | % Carbon from the atmosphere (based on carbon isotope ratios) |
|---|---|---|---|---|
| K3 | 1.5 | −12.00 | −12.37 | 35.7 |
| T1 | 1.6 | −10.90 | −10.67 | 32.4 |
| S1 | 9.4 | −12.40 | −11.38 | 36.9 |
| M4 | 44.7 | −7.48 | −8.03 | 22.2 |
| M10 | 85.9 | −12.80 | −9.49 | 38.1 |
| R2 | 105.5 | −3.54 | −9.36 | 10.5 |
| MD1 | 110.0 | −5.17 | −8.82 | 15.4 |

**Table 4**
PHREEQC model input/output of red mud solution chemistry reported (R) in Mayes et al. (2011) and CSIRO (2009) and after the solution is modelled in equilibrium with gypsum (G).

| | Mayes et al., (2011) | | | | | | CSIRO (2009) | |
|---|---|---|---|---|---|---|---|---|
| | K1-R | K1-G | K2-R | K2-G | K3-R | K3-G | R | G |
| pH | 13.06 | 12.88 | 10.50 | 10.29 | 10.08 | 9.86 | 10.66 | 10.20 |
| Temp (°C) | 3.60 | | 4.20 | | 3.90 | | 20.00 | |
| $\mu mol\ L^{-1}$ | | | | | | | | |
| Ca | 37.82 | 18510 | 2.22 | 13820 | 0.94 | 13780 | 47.48 | 19100 |
| $SO_4$ | 7.57 | 18480 | 2.95 | 13820 | 2.71 | 13780 | 1772 | 20830 |
| SI Gypsum | −5.74 | 0.00 | −6.63 | 0.00 | −7.03 | 0.00 | −3.59 | 0.00 |
| SI Aragonite | −1.46 | 0.53 | −2.99 | −0.28 | −3.50 | −0.30 | 0.62 | 2.77 |
| SI Calcite | −1.29 | 0.69 | −2.83 | −0.12 | −3.34 | −0.14 | 0.77 | 2.92 |

neutralisation. Other buffering alternatives, such as direct carbonation (which suffers from transient buffering effects; Khaitan et al., 2009) and microbial buffering (see Gräfe et al., 2011 for detail) represent other means to develop sustainable treatment technologies for hyperalkaline red mud leachates, particularly at disposal sites in temperate climate zones where leachate generation can pose an enduring problem and acid dosing is not economically viable over the long term. However, the broader ecological effects of gypsum addition may warrant further investigation. In analogous systems receiving hyperalkaline calcareous waters, numerous deleterious effects have been noted. These include (1) the effects of extensive benthic smothering and rapid rates of carbonate deposition (e.g. Koryak et al., 2002), (2) poor physical structure of secondary calcareous deposits (Auer et al., 1996; Madsen et al., 1996) and (3) the formation of hardpans, which prevent root penetration under low flow conditions (Mayes et al., 2009).

## Acknowledgements

We are grateful to the UK Natural Environment Research Council for funding the work (grant NE/I019468/1). We are indebted to Bob Knight (University of Hull) and Jane Davis (Newcastle University) for analyses. We also thank Viktória Feigl, Orsolya Klebercz, Mária Tolner, Ermese Vaszita (Budapest University of Technology and Economics) for field support; Gyozo Jordan (Geological Institute of Hungary), Kovacs Laszlo and István Csonki (Central Danubian Water and Environment Authority) for site information; and Krisztina Kocsis (British Embassy) for facilitating site access. We would like to thank Markus Gräfe and an anonymous reviewer for insightful comments that have improved the manuscript.

## References

Andrews JE, Gare SG, Dennis PF. Unusual isotopic phenomena in Welsh quarry water and carbonate crusts. Terra Nova 1997;9:67–70.
Auer MT, Johnson NA, Penn MR, Effler SW. Pollutant sources, depositional environment and the surficial sediments of Onondaga Lake, New York. J Environ Qual 1996;25:46–55.
Bajnóczi B, Kovács-Kis V. Origin of pedogenic needle-fiber calcite revealed by micromorphology and stable isotope composition—a case study of a Quaternary paleosol from Hungary. Chem Erde Geochem 2006;66:203–12.
Ball JW, Nordstrom DK. User's manual for WATEQ4F with revised thermodynamic database and test cases for calculating speciation of major, trace and redox elements in natural waters. U.S. Geological Survey Water Resources Investigation, Report; 1991. p. 91-183.
Benedek J, editor. The Kolontár Report: Causes and Lessons from the Red Mud Disaster. Budapest: Sustainable Development Committee of the Hungarian Parliament; 2011.
Burke IT, Mayes WM, Peacock CL, Brown AP, Jarvis AP, Gruiz K. Speciation of contaminant metals in red mud samples from the Ajka spill site, Hungary. Mineralog Mag 2011;75(3):599.
Clark ID, Fontes J-C, Fritz P. Stable isotope disequilibria in travertine from high pH waters: laboratory investigations and field observations from Oman. Geochim Cosmochim Acta 1992;56:2041–50.
Courtney RG, Timpson JP. Reclamation of fine fraction bauxite processing residue (red mud) amended with coarse fraction residue and gypsum. Water Soil Air Pollut 2005;164:91-102.
CSIRO. Characterisation of mining and industrial by-products with potential for use as environmental amendments. Western Australia Water Foundation; 2009. ISSN: 1835-095X.
Dietzel M, Usdowski E, Hoefs J. Chemical and $^{13}C/^{12}C$- and $^{18}O/^{16}O$-isotope evolution of alkaline drainage waters and the precipitation of calcite. Appl Geochem 1992;7:177–84.
European Commission Monitoring and Information Centre for Civil Protection. Alkali sludge depository dyke breach in Kolontár, Veszprém County, Hungary Situation Report 3. European Union; 2010. October 6th.
Fléhoc C, Girard JP, Piantone P, Bodénan F. Stable isotope evidence for the atmospheric origin of $CO_2$ involved in carbonation of MSWI bottom ash. Appl Geochem 2006;21:2037–48.
Gelencsér A, Kováts N, Turóoczi B, Rostási Á, Hoffer A, Imre K, et al. The red mud accident in Ajka (Hungary): characterization and potential health effects of fugitive dust. Environ Sci Technol 2011;45:1608–15.
Gräfe M, Klauber C. Bauxite residue issues: IV. Old obstacles and new pathways for in-situ bioremediation. Hydrometallurgy 2011;108:46–59.
Gräfe M, Power G, Klauber C. Bauxite residue issues: III. Alkalinity and associated chemistry. Hydrometallurgy 2011;108:60–79.
Gruiz K. Environmental Information: The red mud catastrophe in Hungary. http://enfo.agt.bme.hu/drupal/en/gallery/808120102010.
Harnisch JI, Wing Sue, Jacoby HD, Prinn RG. Primary aluminum production: climate policy, emissions and costs, MIT JPSPGC Report No. 44, December. also Extraction and Processing Division Congress 1999. The Minerals Metals and Materials Society; 1998http://web.mit.edu/globalchange/www/rpt44.html.
Hudson JD. Stable isotopes and limestone lithification. J Geol Soc 1977;133(6):637–60.
Hungarian Ministry of Foreign Affairs. Information on the accidental pollution and related mitigation measures of the "red mud spill at Ajka". http://www.mfa.gov.hu/kulkepviselet/CZ/en/en_Hirek/V%C3%B6r%C3%B6siszap_en.htm?printable=-true2010. [ last accessed: 07.07.2011].
Johnston M, Clark M, McMahon P, Ward N. Alkalinity conversion of bauxite refinery residues by neutralization. J Hazard Mater 2010;182:710–5.
Khaitan S, Dzombak DA, Lowry GV. Neutralization of bauxite residue with acidic fly ash. Environ Eng Sci 2009;26:431–40.
Koryak M, Stafford LJ, Reilly RJ, Magnuson MP. Impacts of steel mill slag leachate on the water quality of a small Pennsylvania stream. J Freshw Ecol 2002;17:461–5.
Kosednar-Legenstein B, Dietzel M, Leis A, Stingl K. Stable carbon and oxygen isotope investigation in historical lime mortar and plaster — results from field and experimental study. Appl Geochem 2008;23:2425–37.
Krishnamurthy RV, Schmitt D, Atekwana EA, Baskaran M. Isotopic investigations of carbonate growth on concrete structures. Appl Geochem 2003;18:435–44.
Leoni F, Penco C. Bauxite residue desulphurisation system (BRDS) at Eurallumina. In: Chandrashekar S, editor. Proceedings of the 6th International Alumina Quality Workshop. Brisbane: AQW Inc.; 2002.
Létolle R, Gégout P, Moranville-Regourd M, Gaveau B. Carbon-13 and oxygen-18 mass spectrometry as a potential tool for the study of carbonate phases in concretes. J Am Ceram Soc 1990;73:3617–25.
Liu Y, Lin C, Wu Y. Characterization of red mud derived from a combined Bayer Process and Calcining method for alumina refining. Chin J Geochem 2007;25:40. (0).
Macleod G, Fallick AE, Hall AJ. The mechanism of carbonate growth on concrete structures, as elucidated by carbon and oxygen isotope analyses. Chem Geol 1991;86:335–43.
Madsen JD, Bloomfield JA, Sutherland JW, Eichler LW, Boylen CW. The aquatic macrophyte community of Onondaga Lake: field survey and plant growth bioassays of lake sediments. Lake Reserv Manage 1996;12:73–9.
Mayes WM, Batty LC, Younger PL, Jarvis AP, Kõiv M, Vohla C, et al. Wetland treatment at extremes of pH — a review. Sci Total Environ 2009;407:3944–57.
Mayes WM, Jarvis AP, Burke IT, Walton M, Feigl V, Klebercz O, et al. Dispersal and attenuation of trace contaminants downstream of the Ajka bauxite residue (red mud) depository failure, Hungary. Environ Sci Technol 2011;45:5147–55.
O'Neil JR, Barnes I. $C^{13}$ and $O^{18}$ compositions in some fresh-water carbonates associated with ultramafic rocks and serpentinites: western United States. Geochim Cosmochim Act 1971;35:687–97.
Pálfy J, Demény A, Haas J, Hetényi M, Orchard MJ, Veto I. Carbon isotope anomaly and other geochemical changes at the Triassic–Jurassic boundary from a marine section in Hungary. Geology 2001;29:1047–50.
Parkhurst DL, Appelo CAJ. User's guide to PHREEQC—a computer program for speciation, batch-reaction, one-dimensional transport, and inverse geochemical calculations. U.S. Geological Survey Water-Resources Investigations Report; 1999. p. 99-4259.
Power G, Gräfe M, Klauber C. Bauxite residue issues: I. Current management, disposal and storage practices. Hydrometallurgy 2011;108:33–45.
Reeves HJ, Wealthall G, Younger PL. Advisory visit to the bauxite processing tailings dam near Ajka, Veszprém County, western Hungary. British Geological Survey, Keyworth, UK. Open Report OR/11/006; 2011.
Renforth P, Manning DAC, Lopez-Capel E. Carbonate precipitation in artificial soils as a sink for atmospheric carbon dioxide. Appl Geochem 2009;24:1757–64.
Renforth P, Washbourne CL, Taylder J, Manning DAC. Silicate production and availability for mineral carbonation. Environ Sci Technol 2011;45:2035–41.
Roadcap GS, Kelly WR, Bethke CM. Geochemistry of extremely alkaline (pH >12) ground water in slag-fill aquifer. Ground Water 2005;43:806–16.
Robie RA, Hemingway BS. Thermodynamic properties of minerals and related substances at 298.15 K and 1 bar (105 Pascals) pressure and at higher temperatures. In United States Geological Survey Bulletin 2131; WA; 1995.
Ruyters S, Mertens J, Vassilieva E, Dehandschutter B, Poffijn A, Smolders E. The red mud accident in Ajka (Hungary): plant toxicity and trace metal bioavailability in red mud contaminated soil. Environ Sci Technol 2011;45:1616–22.
Tessier A, Campbell PGC, Bisson M. Sequential extraction procedure for the speciation of particulate trace metals. Anal Chem 1979;51:844–51.
The Royal Society. Geoengineering the climate: science, governance and uncertainty. London, UK: The Royal Society; 2009.
Usdowski E, Hoefs J. 13C/12C partitioning and kinetics of CO2 absorption by hydroxide buffer solutions. Earth Planet Sci Lett 1986;80:130–4.
USEPA. Microwave assisted acid digestion of siliceous and organically based matrices. Method 1996;2052.
USGS. United States Geophysical Survey Minerals Yearbook. U.S. Department of the Interior and U.S. Geological Survey; 2010.
USGS. United States Geophysical Survey Minerals Commodity: Aluminium, U.S. Department of the Interior and U.S. Geological Survey; 2011. Available athttp://minerals.usgs.gov/minerals/pubs/commodity/aluminum/mcs-2011-alumi.pdf.

Van Strydonck MJY, Dupas M, Keppens E. Isotopic fractionation of oxygen and carbon in lime mortar under natural environmental conditions. Radiocarbon 1989;31: 610–8.
Wehr JB, Fulton I, Menzies NW. Revegetation strategies for bauxite refinery residue: a case study of Alcan Gove in Northern Territory, Australia. Environ Manage 2006;37:297–306.
Yadav VS, Prasad M, Khan J, Amritphale SS, Singh M, Raju CB. Sequestration of carbon dioxide ($CO_2$) using red mud. J Hazard Mater 2010;176:1044–50.
Yamada K, Harato F. $SO_2$ removal from waste-gas by red mud slurry pilot test and operation results of the plant. Kagaku Kogaku Ronbunshu 1982;8:32–8.